Boundary-Layer Meteorol (2011) 140:87–103
DOI 10.1007/s10546-011-9598-0

ARTICLE

A Lagrangian Model to Predict the Modification of Near-Surface Scalar Mixing Ratios and Air–Water Exchange Fluxes in Offshore Flow

Mark D. Rowe · Judith A. Perlinger · Christopher W. Fairall

Received: 1 May 2010 / Accepted: 7 February 2011 / Published online: 10 March 2011

Abstract A model was developed to predict the modification with fetch in offshore flow of mixing ratio, air–water exchange flux, and near-surface vertical gradients in mixing ratio of a scalar due to air–water exchange. The model was developed for planning and interpretation of air–water exchange flux measurements in the coastal zone. The Lagrangian model applies a mass balance over the internal boundary layer (IBL) using the integral depth scale approach, previously applied to development of the nocturnal boundary layer overland. Surface fluxes and vertical profiles in the surface layer were calculated using the NOAA COARE bulk algorithm and gas transfer model (e.g., Blomquist et al. 2006, Geophys Res Lett 33:1–4). IBL height was assumed proportional to the square root of fetch, and estimates of the IBL growth rate coefficient, α, were obtained by three methods: (1) calibration of the model to a large dataset of air temperature and humidity modification over Lake Ontario in 1973, (2) atmospheric soundings from the 2004 New England Air Quality Study and (3) solution of a simplified diffusion equation and an estimate of eddy diffusivity from Monin–Obukhov similarity theory (MOST). Reasonable agreement was obtained between the calibrated and MOST values of α for stable, neutral, and unstable conditions, and estimates of α agreed with previously published parametrizations that were valid for the stable IBL only. The parametrization of α provides estimates of IBL height, and the model estimates modification of scalar mixing ratio, fluxes, and near-surface gradients, under conditions of coastal offshore flow (0–50 km) over a wide range in stability.

M. D. Rowe · J. A. Perlinger (✉)
Department of Civil and Environmental Engineering, Michigan Technological University,
1400 Townsend Dr., Houghton, MI 49931, USA
e-mail: jperl@mtu.edu

Present Address:
M. D. Rowe
Large Lakes and Rivers Forecasting Research Branch, U.S. Environmental Protection Agency,
9311 Groh Rd., Grosse Ile, MI 48138, USA

C. W. Fairall
Earth System Research Laboratory, National Oceanic and Atmospheric Administration,
325 Broadway, Boulder, CO 80303, USA

Keywords Air–sea gas exchange · Bulk Richardson number · Internal boundary layer · Offshore flow · Stability

List of Symbols

dT_a	Land–lake air temperature modification
dT_d	Land–lake dewpoint temperature modification
f	Fraction of h that defines the top of the surface layer
F	Flux per unit area at the surface
g	Acceleration due to gravity
$H(x)$	Integral depth scale
$H(x)_u$	Upper portion of the integral depth scale above the surface layer
$H(x)_l$	Lower, surface-layer portion of the integral depth scale
h	Height of the internal boundary layer
K	Turbulent eddy diffusivity
k_a	Atmospheric gas transfer velocity
L	Obukhov length
n	Exponent that determines the shape of the IBL mixing ratio profile
P	Atmospheric pressure
R	Gas constant
Ri_b	Bulk Richardson number
Ri_{b10}	Bulk Richardson number defined using upstream, overland meteorological Variables at 10-m reference height
$r(z)$	Gas mixing ratio as a function of height
r_l	Upstream, overland mixed layer gas mixing ratio
r_s	Gas mixing ratio at the surface
T	Absolute temperature
U	Mean wind speed in the x direction
U_{10}	Wind speed at 10-m height
$\overline{U}$	Wind speed averaged vertically over the IBL
u_*	Friction velocity
x	Horizontal dimension aligned with the mean wind
X	Fetch: distance travelled by the air mass over water from the coast
z	Vertical dimension, positive upward
z_m	Profile matching height; border between the surface layer and the IBL
z_o	Aerodynamic roughness length
z_r	Reference height at which wind speed or scalar has a known value
α	IBL growth rate coefficient
γ	Lapse rate: deviation of temperature or mixing ratio vertical profile from well-mixed condition
γ_d	Dry adiabatic lapse rate, $\gamma_d = -0.0098\,\mathrm{K\,m^{-1}}$
γ_e	Environmental lapse rate
θ	Potential temperature
θ_v	Virtual potential temperature
θ_{vl}	Upstream, overland mixed layer θ_v
θ_{vs}	θ_v of air at equilibrium with the water surface
κ	von Kármán constant, assumed to have a value of 0.4
$\Phi_H(z/L)$	MOST gradient profile function for potential temperature
$\Psi_M(z/L)$	MOST integral profile function for wind speed

1 Introduction

The quantification of air–water exchange fluxes of trace gases, such as carbon dioxide (McGillis et al. 2004), dimethyl sulphide (Blomquist et al. 2006), and semivolatile organic compounds (Perlinger et al. 2005, 2008) is important for our understanding and predicting climate change and ecosystem health. Measurements of air–water exchange fluxes in the coastal zone are conducted within a complex environment of an evolving internal boundary layer (IBL) as air advected from land adjusts to the change in surface forcing caused by flow over the water surface. Bulk algorithms that assume horizontal homogeneity may not agree with flux measurements made at a significant fraction of the IBL height (Fairall et al. 2006).

A model framework is necessary to plan and interpret coastal air–water exchange flux measurements, to evaluate the reasonableness of flux measurements, and to predict the values of fluxes as a function of bulk meteorological variables. Models of IBL development range from complex numerical turbulence models (Garratt 1987; Smedman et al. 1997; Angevine et al. 2006b) to relatively simple Lagrangian models (Garratt 1987; Hsu 1989; Melas 1989). Angevine et al. (2006b) applied a high-resolution numerical model to investigate pollutant transport in offshore, coastal flow associated with the 2002 New England Air Quality Study, and found that some, but not all, of the important phenomena were captured: the stable boundary layer predicted by the model formed further from shore, was less stable, and was thicker than observations. Fine-scale phenomena near the coast can be challenging for numerical models to capture as IBL growth is difficult to establish from first principles, and so empirical formulae are often used. For example, Mulhearn (1981) provided a simple relation for IBL depth applicable for the stable surface layer. Previous investigations of IBL formation in coastal offshore flow focused primarily on the thermal IBL under stable conditions. The full range of stable, neutral, and unstable conditions is of interest with respect to air-surface exchange of trace gases. The objective of this article is to develop a simple model to predict the modification of scalar mixing ratio, fluxes, and near-surface gradients resulting from air–water exchange in coastal offshore flow over a wide range in stability, which is useful for the planning and interpretation of coastal air–water exchange flux measurements.

We apply the coupled ocean-atmosphere response experiment (COARE) bulk algorithm (Fairall et al. 2003) and gas transfer model (Fairall et al. 2000; Blomquist et al. 2006) within a Lagrangian framework, referred to in this article as the internal boundary-layer transport and exchange (IBLTE) model, to estimate the height to which an air mass is modified by the water surface in offshore flow (i.e., the height of the IBL), and to estimate the modification of gas mixing ratio, potential temperature, surface fluxes, and near-surface vertical profiles with fetch. We develop a parametrization to quantify IBL growth under stable, neutral, and unstable conditions by calibration of the IBLTE model to observations of air temperature and humidity modification in offshore flow, and compare to a parametrization based on Monin–Obukhov similarity theory (MOST) and previously published parametrizations that are valid only for the stable IBL.

2 Model Description

An IBL forms in the atmosphere whenever flow passes over a change in surface properties such as roughness, temperature, or moisture (Garratt 1990). Except in nearly calm or very unstable conditions, the influence of the new surface is propagated upward by turbulent diffusion more slowly than it is advected horizontally, and thus, some time (distance) is required to establish new steady-state vertical profiles of temperature and mixing ratio (Fig. 1).

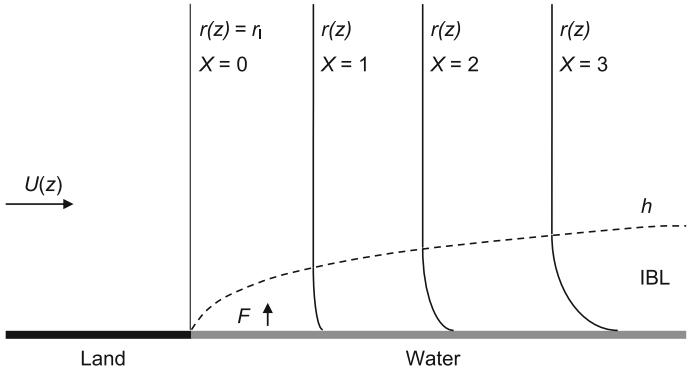

Fig. 1 Modification of the vertical profile of the gas mixing ratio, r, with increasing fetch, X, as a well-mixed atmospheric boundary layer is advected from land to water with a gas flux directed upward from the surface. The internal boundary layer is defined as the height to which mixing ratio is modified through exchange with the surface

In the case of cool air flowing over a warmer surface, a statically unstable or convective IBL is formed. Turbulence is enhanced by convection, and thus, the convective IBL grows rapidly and reaches equilibrium in tens of kilometres (Garratt 1987). In contrast, when warm air flows over a cooler surface, turbulence is suppressed by thermal stratification and a statically stable IBL is formed. The growth rate of a stable IBL is low, and a fetch of several hundred kilometres is required to develop an IBL of several hundreds of metres deep (Garratt 1987).

2.1 A Mass/Heat Balance Over the Internal Boundary Layer

A mass balance is performed over the IBL taking a Lagrangian perspective, moving with an air mass advected from land to water in a direction aligned with the mean wind. The IBL is defined as the vertical distance above the water surface that is affected by exchange with the surface. The IBL grows by entrainment of air from above, which is assumed to be unmodified from the original vertical profiles of scalar quantities incident at the coast. The IBLTE model assumes non-zero mean wind speed, an initial scalar profile incident at the coast that is constant or linear (increasing or decreasing) with height, neglects directional wind shear, subsidence, and body sources. Sea-surface temperature and dissolved gas concentration are assumed constant with fetch.

The mass balance is written by setting the vertical integral of the profile modification equal to the horizontal integral of flux through the surface at the fetch of interest. This approach yields a quantity with units of length, $H(x)$, which is called the integral depth scale (Stull 1988):

$$H(x) \equiv \int_0^h (r(z) - r_1)\,\mathrm{d}z = \int_0^X \frac{F}{\overline{U}} \frac{RT}{P} \mathrm{d}x \tag{1}$$

where h is the height of the IBL, $r(z)$ is the mixing ratio as a function of height at the fetch of interest, r_1 is the mixing ratio overland (assumed to be constant or a linear function of z), F is the flux at the surface, $\overline{U}$ is the wind speed averaged vertically over the IBL, R is the gas constant, T is the average absolute air temperature, P is the atmospheric pressure, and x is the horizontal dimension aligned with fetch (see the full list of symbols). The concept of

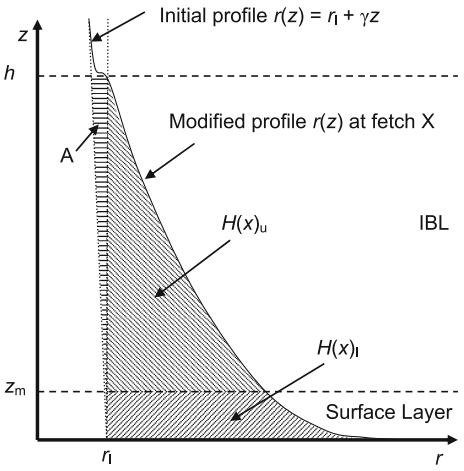

Fig. 2 Modification of the vertical profile of gas mixing ratio within the internal boundary layer in an air mass advected from land to water at a specific fetch, X. In this scenario, the initial mixing ratio profile overland is $r(z) = r_l + \gamma z$ and there is an upward gas flux from the water. The regions $H(x)_u$, $H(x)_l$, and A correspond to components of the mass balance discussed in the text and in Appendix A

performing a mass balance by integration of the scalar profile modification over the IBL is illustrated in Fig. 2.

Once the integral depth scale has been determined by evaluating the horizontal integral in Eq. 1, the modification to the mixing ratio as a function of height can be found if profile functions are defined. To this end, a relatively thin surface layer is defined within the IBL where the flux can be assumed to depart minimally from the surface value, F, and thus the stability-dependent MOST profile functions used in the COARE algorithm apply. This approach is modelled after the concept of Mahrt (1999, Fig.1), which indicates that the height within the IBL over which z/L (MOST) scaling is appropriate decreases with increasing stability. Over the remainder of the IBL, above the constant-flux surface layer, the IBL profile function of Garratt (1990), z/h scaling, is applied, as illustrated in Fig. 2.

The approach to evaluate the vertical integral in Eq. 1 begins with specifying h. The magnitude of h is assumed to increase as the square root of fetch, X:

$$h = \alpha X^{0.5} \tag{2}$$

where Garratt (1990) reported that the square-root-of-fetch dependence is a reasonable approximation for both the stable and unstable IBL. At long fetch, h approaches a limiting value, and Eq. 2 no longer applies. The studies cited by Garratt (1990) are generally limited to $X < 100$ km for stable cases, and $X < 50$ km for unstable cases. In any case, h predicted by Eq. 2 should be limited to values less than the depth of the mixed layer advected from land. The parametrization of α as a function of the bulk Richardson number is discussed subsequently.

The depth of the constant-flux layer is defined as a constant fraction of h:

$$z_m = fh \tag{3}$$

where z_m is the matching height at which the surface layer and IBL profile functions match, and f is a fraction of the IBL height. A value of 0.1 was selected for f. Evidence for $f = 0.1$ can be found in, e.g., Fairall et al. (2006, Fig. 9), where it is shown that the momentum flux measured at 18-m height is representative of the expected surface flux when h exceeds 200 m.

Within the surface layer, vertical profiles of potential temperature and specific humidity are obtained from the MOST profile functions in the COARE algorithm. For gas mixing ratio, a vertical profile is constructed through use of the atmospheric transfer velocity given by the COARE algorithm (after Fairall et al. 2000; Blomquist et al. 2006):

$$r(z) = r_{z_r} + \frac{RT}{P} F_s \left[\frac{1}{k_{az_r}} - \frac{1}{k_{az}} \right] \tag{4}$$

where $r(z)$ is the mixing ratio at the height of interest, r_{z_r} is the known value of the mixing ratio at some reference height, and k_{az_r} and k_{az} are the atmospheric transfer velocities for the gas of interest at the reference height and the height of interest, respectively.

Within the range $z_m < z < h$, the vertical profile of mixing ratio or potential temperature is described by the IBL dimensionless profile function of Mulhearn (1981):

$$\frac{(r - r_s)}{(r_1 - r_s)} = \left(\frac{z}{h}\right)^n \tag{5}$$

where r_s is the mixing ratio at the surface. As it is applied here, r_s does not correspond to the value of the mixing ratio at the surface because the (z/h) profile is only applied above z_m. The value of r_s is determined so that the profiles described by Eqs. 4 and 5 match at z_m, as described in Appendix A. The exponent n is a constant that determines the shape of the profile. For the stable, thermal IBL, Garratt (1990, p. 196) cited earlier studies that found $n = 0.25$ at $X \approx 30$ km and $n = 2$ for $45 < X < 300$ km, and speculated that the profile curvature changes rapidly at short fetch. Analysis of 35 profiles from NEAQS (explained subsequently) at $2\,\text{km} < X < 190\,\text{km}$ did not reveal a consistent value of n for short or long fetch. A value of $n = 1$ was selected for stable and neutral conditions, while a value of $n = 10$ was found to give a slightly better fit to air temperature and humidity modification data for unstable conditions in the calibration. The IBL profile function, Eq. 5, serves as a means to close the mass balance over the IBL by providing a transition from the MOST profile to the unmodified profile advected from land, but is not expected to accurately predict scalar mixing ratios and gradients above z_m. This is consistent with the objective of the IBLTE model, which is to predict the modification of fluxes, mixing ratio, and vertical gradients within the constant-flux layer where the MOST profiles are valid ($z < 0.1h$). Additional mathematical details of the model are provided in Appendix A.

2.2 Estimation of the IBL Growth Rate Coefficient from Air Temperature and Humidity Modification Data

The IBL growth rate coefficient, α, was calibrated using a large dataset of over-water temperature and humidity modification (Phillips and Irbe 1978). The data of Phillips and Irbe are unique in spatial and temporal coverage, although they do not directly quantify IBL height. Thus, we used the IBLTE model in an iterative process to find values for α that best fit the temperature and humidity modification data. The dataset, derived from 6,926 pairs of land and over-water measurements of temperature, dewpoint temperature, and wind speed, was collected over the 12-month period of the International Field Year of the Great Lakes, 1973, using an array of 20 data buoys installed on Lake Ontario especially for the purpose. The data cover a range in wind speed, air–water temperature difference, and stability, which are representative of an annual cycle over the Great Lakes. The data were reported in the form of the average, standard deviation, and number of measurements of air temperature and dewpoint temperature modification for measurements grouped into classifications

of overland wind speed, overland air–water temperature difference, and fetch. Empirical correlations derived from the same dataset are currently used for adjusting overland meteorological data for over-water modification in an evaporation model for the Great Lakes (Croley II 1989).

To calibrate α using the IBLTE model, it was necessary to compile a set of overland meteorological data that were representative of the overland meteorological data of Phillips and Irbe, which are no longer available. Phillips and Irbe (1978) classified the data based on stability, characterized by air–water temperature difference at the coast, and wind speed. Stability is more correctly indicated by the Richardson number than by air–water temperature difference alone. Some of the 30 Phillips and Irbe classes of air–water temperature difference and wind speed covered a wide range of Richardson number. The 10-m bulk Richardson number was used here for characterizing stability at the coast:

$$Ri_{\mathrm{b10}} = \frac{g10(\theta_{\mathrm{vl}} - \theta_{\mathrm{vs}})}{\theta_{\mathrm{vl}} U_{10}^2} \tag{6}$$

where θ_{vl} and θ_{vs} are the virtual potential temperatures of the mixed layer overland and of air at equilibrium with the water surface, respectively, U_{10} is the 10-m wind speed overland, and g is the acceleration due to gravity.

An objective in compiling the calibration set of meteorological conditions was to simulate as closely as possible the distribution of Richardson numbers, as well as the actual ranges of meteorological conditions, within each of the Phillips and Irbe classes. To this end, historical data for Lake Ontario, 1973, were obtained from the Toronto International Airport (Environment Canada 2009), one of the stations used by Phillips and Irbe, to obtain overland air temperature, dewpoint temperature, and wind speed. Monthly mean water-surface temperatures (Croley and Hunter 1996) for Lake Ontario, 1973 were interpolated to the hourly data from Toronto.

A calibration dataset of 937 sets of input data was compiled by randomly selecting records from the time series on the synoptic hours (0600, 1200, 1800, and 0000 UTC), then assigning them to the 30 Phillips and Irbe classes. Phillips and Irbe also sampled their data only on the synoptic hours. The number of records assigned to a class was arbitrarily capped at 50, which was considered to produce a representative sample while maintaining a reasonable model calibration time (approximately 6 h). The median Ri_{b10} value and calibrated value of α for each class was not sensitive to repeated random samples. All the records in the time series were used for 22 of 30 classes because the time series, sampled on the synoptic hours, contained fewer than 50 records. These classes represent relatively infrequent meteorological events. Furthermore, since all of the synoptic hour records were used for 22 of the 30 classes, it is likely that many of these records represent the same relatively infrequent meteorological events from 1973 that were sampled by Phillips and Irbe.

To indicate the frequency of occurrence of the values of Ri_{b10}, frequency distributions of Ri_{b10} from the time series are presented in Table 1. The frequency of occurrence of Ri_{b10} values decreases rapidly with increasing absolute value of Ri_{b10}. Sampling the time series on the synoptic hours resulted in a similar frequency distribution to the full dataset. The calibration set captured all of the extreme values of the synoptic hour sample, and a random sub-sample of the frequently occurring values.

To obtain a calibrated value of α for each class, the model was run repeatedly for each record in the calibration dataset using a routine to find the value of α that minimized the sum of the squared errors, inverse weighted by the standard error of the Phillips and Irbe data, between modelled and measured air temperature and dewpoint temperature modification.

Table 1 Frequency distribution of the 10-m bulk Richardson number based on hourly meteorological data from Toronto and interpolated water surface temperatures for Lake Ontario for 1 January to 31 December, 1973

Percentile rank	Toronto 1973 all hours	Toronto 1973 synoptic hours	Calibration set
Maximum	13.8	13.8	13.8
99	1.83	1.76	2.28
95	0.390	0.451	0.667
75	0.0652	0.0590	0.0578
Median	−0.0080	−0.0087	−0.0200
25	−0.117	−0.125	−0.146
5	−0.782	−0.834	−1.18
1	−2.75	−3.33	−4.96
Minimum	−22.0	−11.4	−11.4
n	8760	1759	937

Upon completion of the calibration, the median of the several values of α within each class was taken to obtain a single value of α for each class.

To verify the calibration, the model was run for the calibration dataset, using the median value of α for each class, and the root-mean-square (r.m.s.) errors for air temperature and dewpoint temperature modification were calculated; the r.m.s. errors were 1.3 and 1.6°C, respectively. Modelled and measured air temperature and dewpoint temperature modification for the 30 Phillips and Irbe classes and for each record in the calibration set of meteorological data are shown in Figs. 3 and 4, respectively.

2.3 Estimation of the IBL Growth Rate Coefficient from Atmospheric Soundings

Rawinsonde profiles collected off the east coast of North America as part of the 2004 New England Air Quality Study (NEAQS) (Fairall et al. 2006; Angevine et al. 2006a) provide additional estimates of α. The NEAQS rawinsonde profiles were used to estimate values of α using Eq. 2 with h estimated from the sounding and the fetch estimated using a HYSPLIT model (Draxler et al. 2009) backward air parcel trajectory. First, 48 soundings were selected from the maps described by Fairall et al. (2006) that had wind vectors at 17.5-m and 250-m heights that both indicated flow from land. HYSPLIT backward trajectories were run for each of these soundings (24 h, 10-m starting height, constant pressure height, FNL archived meteorological data). Several soundings were then eliminated because flow from the sea was indicated by the back-trajectory, leaving 35 soundings. The fetch was summed along the back trajectory from the location where the trajectory crossed the coast.

The IBL height, h, was estimated from the sounding by the mixing diagram approach (Craig 1946; Angevine et al. 2006a) as well as by using an Ri_{b} threshold of 0.10, 0.25, and 0.50, as was done by Fairall et al. (2006). Upstream, overland meteorological variables needed to calculate Ri_{b10} values for the NEAQS soundings were obtained from the sounding data using temperature and humidity taken from the next level above h in the sounding (assumed to be unmodified over the fetch), and the 10-m wind speed was calculated using the stability-dependent MOST relationship after calling the COARE algorithm with inputs from the second level in the rawinsonde data (change in wind speed on movement of the air

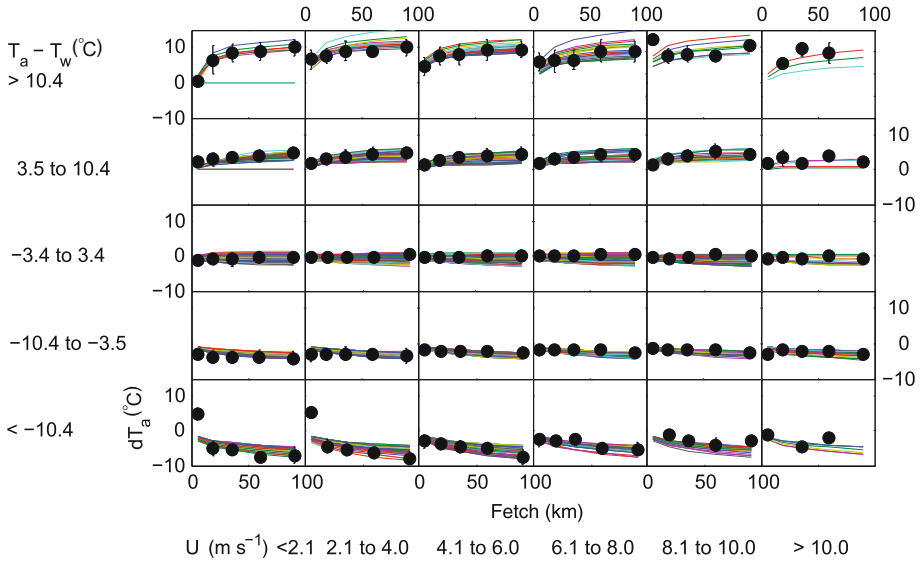

Fig. 3 Results of calibration of the IBLTE model to observations of land–lake air temperature modification, dT_a(°C), by finding the value of the IBL growth rate coefficient, α, for each class that gave the best fit of modelled to measured dT_a. The panels show dT_a versus fetch for the 30 classes of Phillips and Irbe (1978), classified by air–water temperature difference, T_a–T_w, and wind speed, U, incident at the coast. *Coloured lines* represent the model output for each record in the calibration set of overland meteorological conditions. *Circles* and *error bars* represent the mean and standard error of the binned observations of Phillips and Irbe (1978)

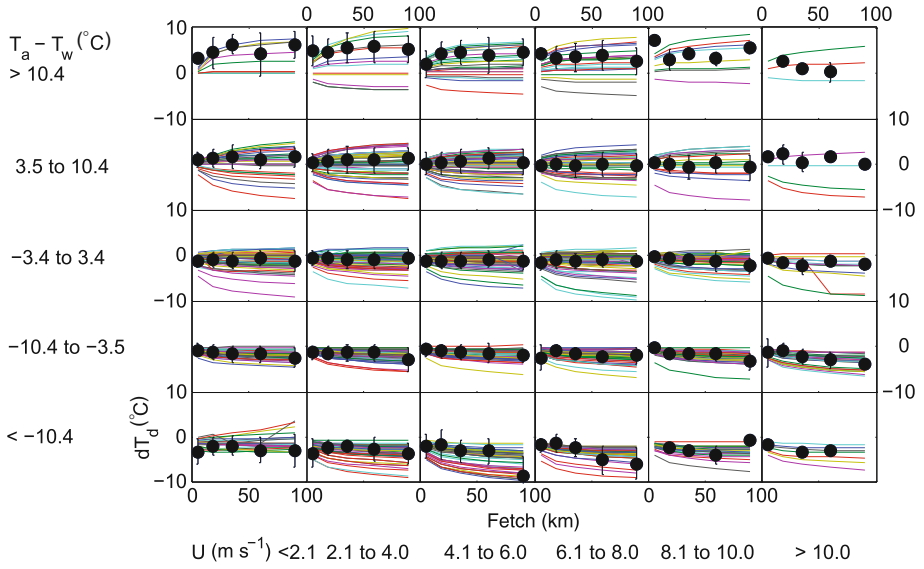

Fig. 4 Same as Fig. 3, but for the dewpoint temperature modification observations of Phillips and Irbe (1978). Each panel in the figure corresponds to a unique value of α, and the same calibrated values of α were used in Fig. 3 as in Fig. 4

mass from land to sea was neglected). The first level in the rawinsonde data was considered to be unreliable because it may have been affected by the ship's wake.

2.4 Parametrization of the IBL Growth Rate Coefficient, α

A parametrization of α is derived here by drawing upon estimates of eddy diffusivity from MOST. There are reasons why MOST may have limited application in the coastal IBL, which are discussed in detail subsequently. Even so, it is interesting to investigate the extent to which the state of turbulence at equilibrium with the water surface can explain estimates of α from observations.

In the simplest case, the modification of temperature or mixing ratio in the IBL can be considered as a function of the rate of horizontal advection and the rate of vertical transport of the thin layer of air equilibrated with the surface. Fick's second law of diffusion is written with the Lagrangian transformation of time to distance as a function of wind speed, U, and turbulent diffusion coefficient, K:

$$U\frac{\partial(\theta-\theta_s)}{\partial x}=K\frac{\partial^2(\theta-\theta_s)}{\partial z^2}. \tag{7}$$

A solution to Eq. 7 for K and U constant in x and z, and for initial and boundary conditions of a uniform mixed layer temperature advected from land, θ_l, and $\theta=\theta_s$ at the surface, is (Taylor 1915; Garratt 1987):

$$(\theta-\theta_s)=(\theta_l-\theta_s)\mathrm{erf}\left(z\left(\frac{U}{4Kx}\right)^{\frac{1}{2}}\right). \tag{8}$$

If the internal boundary-layer height, h, is defined at height z where

$$\frac{(\theta-\theta_s)}{(\theta_l-\theta_s)}=0.9 \tag{9}$$

then Eq. 8 can be re-written as

$$h=2\mathrm{erf}^{-1}(0.9)\left(\frac{K}{U}\right)^{\frac{1}{2}}x^{\frac{1}{2}}, \tag{10}$$

which is equivalent to Eq. 2, where

$$\alpha=2.3\left(\frac{K}{U}\right)^{\frac{1}{2}}. \tag{11}$$

Here the substitution, $2\mathrm{erf}^{-1}(0.9)=2.3$ has been made. To estimate the dependence of α on stability, the stability-dependent forms of the MOST similarity relations are inserted:

$$K=\frac{\kappa z u_*}{\phi_H(z/L)}, \tag{12}$$

$$\frac{u_*}{U}=\frac{\kappa}{\left[\ln\left(\frac{z}{z_0}\right)-\Psi_M\left(\frac{z}{L}\right)\right]}. \tag{13}$$

Combining Eqs. 11, 12, and 13, we obtain

$$\alpha=2.3\kappa\left(\frac{z}{\phi_H\left(\frac{z}{L}\right)\left[\ln\left(\frac{z}{z_0}\right)-\Psi_M\left(\frac{z}{L}\right)\right]}\right)^{\frac{1}{2}}. \tag{14}$$

The gradient profile function for potential temperature, $\phi_H(z/L)$, is used in Eq. 12 because an eddy diffusivity for potential temperature and gas mixing ratio is needed. It is often assumed that K_H and $\phi_H(z/L)$ apply to water vapour and trace gases as well as to potential temperature (Stull 1988, p. 384). The integral profile function for wind speed, $\Psi_M(z/L)$, is used in Eq. 13 because this is a re-arrangement of the stability-dependent wind-speed profile function, used here for obtaining a relationship between the 10-m wind speed and the friction velocity. In Eq. 13, it is appropriate to use $z = 10$ m if U_{10} is used. In Eq. 12, z should be selected to be the height that produces a representative, effective K for the IBL growth, which is unknown, and so $z = 10$ m is used throughout Eq. 14 for the purposes of these calculations. The functions $\phi_H(z/L)$ and $\Psi_M(z/L)$ were taken from the COARE algorithm; original references are cited in Fairall et al. (2003).

3 Results and Discussion

For comparison, the various estimates of α are plotted as a function of Ri_{b10} in Fig. 5. The MOST estimate of α was calculated using Eq. 14 for the set of meteorological data that were used to obtain the calibrated values of α from the Phillips and Irbe (1978) data. The COARE 3.0 algorithm was used to obtain L and z_0 in Eq. 14. The calibrated values of α obtained from application of the IBLTE model to the Phillips and Irbe data are also plotted along with the Mulhearn (1981) parametrization of α, with a constant of 0.02 (Garratt 1990):

$$h = 0.02U\left(\frac{g}{\theta_v}\Delta\theta_v\right)^{-0.5} X^{0.5} = 0.02 z^{0.5} Ri_{bz}^{-0.5} X^{0.5}. \tag{15}$$

Empirical functions having the form

$$\alpha = 0.86\left(\frac{B}{B + Ri_{b10}}\right)^C + (DRi_{b10} + E)\left[1 - \left(\frac{B}{B + Ri_{b10}}\right)^C\right] \tag{16}$$

were fitted to the calibrated values of α (in units of $m^{0.5}$) for stable and unstable conditions, where $0.86\,m^{0.5}$ is the value of Eq. 14 at the limit of neutral stability ($Ri_{b10} = z/L = 0$) and B, C, D, and E are fitting coefficients. For stable conditions ($Ri_{b10} > 0$), $B = 0.0167$, $C = 0.635$, $D = -5.4 \times 10^{-4}$, and $E = 0$ provided a good fit to α calculated from Eq. 14 for the calibration set ($r^2 = 0.982$). For unstable conditions ($Ri_{b10} < 0$), $B = -0.0212$, $C = 0.0957$, $D = 0$, and $E = 7.248\,m^{0.5}$ provided a good fit to α calculated from Eq. 14 for the calibration set ($r^2 = 0.998$). Equation 16 provides a simple means of calculating the MOST estimate of α if it is not convenient to run a bulk algorithm such as COARE to determine z/L and to evaluate the Φ and Ψ functions.

For stable values of Ri_{b10}, there is good agreement among the calibrated values of α, the Mulhearn parametrization, and the MOST estimate of α. Fitting the Mulhearn parametrization to the calibrated values of α results in a coefficient of 0.02, identical to that determined by Garratt (1990), Eq. 15. The coefficient of determination, r^2, was 0.586, indicating that 59% of the variance in the calibrated values of α was explained by the Mulhearn parametrization, and the probability of obtaining an equally high correlation by chance, P, was 0.001. Thus, the approach of obtaining α by calibration of the IBLTE model to the Phillips and Irbe data produced values of α that are consistent with previous investigations in which h was determined from the interpretation of soundings.

While Mulhearn and others were primarily interested in the thermal IBL, which does not exist at the neutral stability limit, the focus here is on the estimation of α for the gas

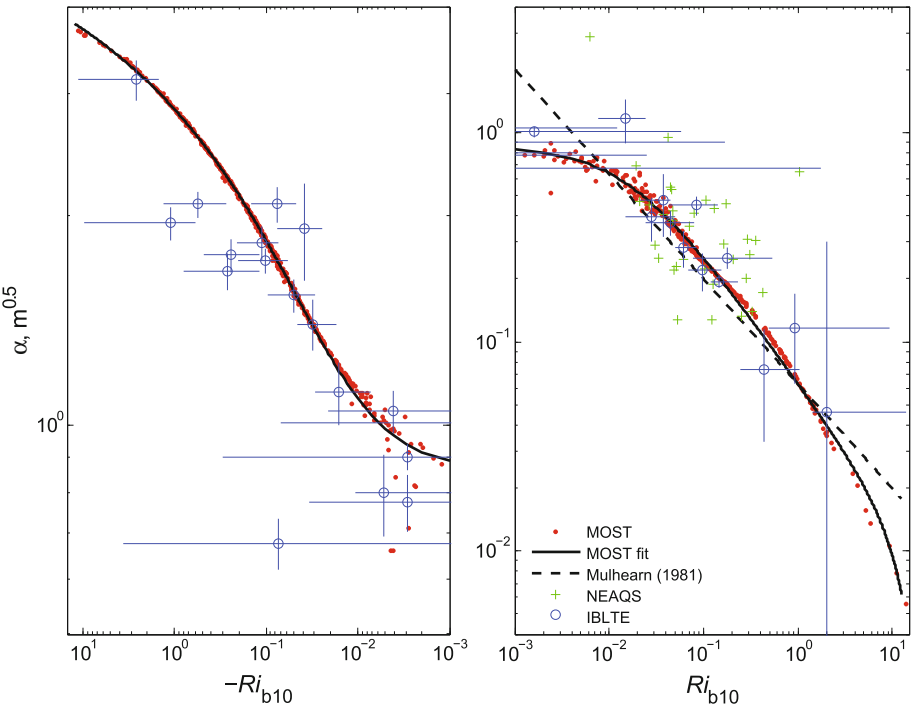

Fig. 5 The IBL growth rate coefficient, $\alpha(\mathrm{m}^{0.5})$, versus the 10-m bulk Richardson number for unstable (*left*) and stable (*right*) conditions. Values of α obtained by calibration of the IBLTE model to the Phillips and Irbe (1978) dataset are plotted as *circles* for each of the 30 classes shown in Figs. 3 and 4. *Vertical error bars* indicate the standard error on the mean of the α values resulting from the range of meteorological conditions in the calibration set for each class. The *horizontal error bar* represents the range in Ri_{b10} from the calibration set that fell within each class. *Horizontal error bars* that cross $Ri_{\mathrm{b10}} = 0$ extend into the other panel of the plot. The symbol is plotted at the median Ri_{b10}. *Red points* represent the MOST estimate of α, Eq. 14, calculated for each record in the calibration set. The *solid black line* is a curve fit to the MOST values of α, Eq. 16. The *dotted black line* is the Mulhearn (1981) parametrization of α, Eq. 15. *Green plus symbols* represent α obtained from the NEAQS soundings

mixing ratio, which means that the entire range of stability is of interest. The Mulhearn (1981) expression approaches infinity as Ri_{b10} approaches zero, which reduced the value of r^2 for the correlation between the Mulhearn expression and the calibrated values of α. Based on the interpretation of α as a function of the eddy diffusivity (Eq. 11), it is intuitive that α should have a finite value at the neutral limit. The average ($\pm$ standard error) of the median values of α calibrated to the neutral Phillips and Irbe classes was $0.87 \pm 0.06\,\mathrm{m}^{0.5}$, which is nearly identical to the value of $0.86\,\mathrm{m}^{0.5}$ that results when Eq. 14 is applied at $z/L = 0$. The MOST estimate of α was more highly correlated to the calibrated values of α than the Mulhearn parametrization for stable conditions, $Ri_{\mathrm{b10}} > 0$ ($r^2 = 0.785$, $P < 0.001$).

The previous literature on the development of the IBL in coastal offshore flow has focused on the stable IBL. The approach of estimating α by calibration of the IBLTE model to the Phillips and Irbe data also allows estimation of α over the unstable range of Ri_{b10}. Very unstable conditions occur during cold air outbreaks in the Great Lakes in late autumn and winter under conditions that are not favourable for field measurements over water. Therefore, the Phillips and Irbe data provide a rare and valuable opportunity to investigate these

conditions. For unstable conditions, the MOST estimate of α was less highly correlated to the calibrated values of α than for stable conditions, but the correlation was still significant ($r^2 = 0.607$, $P < 0.001$).

Values of α estimated from the NEAQS data were weakly correlated to the Mulhearn and MOST estimates of α. The most significant correlation was found when h was determined from the mixing diagram approach ($r^2 = 0.340$, $P < 0.001$), rather than from the critical bulk Richardson number approach of Fairall et al. (2006). The NEAQS data presented challenges in defining h from the rawinsonde profiles and in estimating the upstream meteorological variables overland to calculate Ri_{b10}. The dataset was not as large as that of Phillips and Irbe, and represented individual measurements rather than binned and averaged values that might display less variability. The NEAQS analysis suggests that the values of α derived from the binned and averaged data of Phillips and Irbe may be interpreted as ensemble mean values. Variability in α is expected for individual cases depending on the extent to which the simplifying assumptions made here are met. Furthermore, h, defined as the height to which air has been modified by air–water exchange, is not always distinctly identifiable from features in a sounding. Even so, the IBL concept and parametrization of α are useful to predict the modification of scalar mixing ratios and fluxes with fetch.

A reasonably good correlation was observed between the MOST and Mulhearn parametrizations of α and the calibrated values of α, but there were large discrepancies for some of the Phillips and Irbe classes. The discrepancies could be an artefact resulting from the classification scheme of Phillips and Irbe, or could result from contributions to IBL growth that are not accounted for by the turbulent flow at steady state with the water surface described by MOST. There are several reasons why IBL growth rate may differ from the MOST parametrization: (1) the assumption of U and K constants with z in the MOST derivation is not realistic, and may be less appropriate for unstable than stable conditions because of the greater h; (2) at short fetch, turbulence advected from the land may be more or less intense than the turbulence at steady state with the water surface that is assumed in the MOST estimate of K; (3) turbulence at $z = h$ may be decoupled from the surface under stable conditions; (4) selection of $z = 10$ m to calculate the eddy diffusivity may be less appropriate for unstable than for stable conditions; (5) dependence of h on the square root of fetch is expected to be valid over a limited range of fetch because h approaches a steady-state value at some fetch, which likely occurs at a shorter fetch under unstable conditions than for stable conditions. With these considerations in mind, it is interesting that the MOST parametrization of α is in reasonably good agreement with observations. This finding suggests that bottom-up turbulence generation from the water surface is capable of explaining much of the observed variation in IBL growth rate.

In an effort to investigate whether discrepancies between MOST and calibrated α were caused by the classification scheme of Phillips and Irbe or by variables not accounted for in derivation of the MOST parametrization, the relative error between MOST and calibrated α was analyzed for correlation to other variables. The Phillips and Irbe data were classified by wind speed and air–water temperature difference at the coast, and then averaged. Some of the classes include a wide range in Ri_{b10}, which may have corrupted the dependence of the calibrated α values on Ri_{b10}, particularly for classes in which α has a non-linear Ri_{b10} dependence over the range in Ri_{b10}. There was a weak but significant correlation between relative error in the α estimation and the range in Ri_{b10} normalized to the median Ri_{b10} of the class ($r^2 = 0.392$, $P = 0.050$). The relative error in the α estimation was not significantly correlated to the midpoint wind speed ($r^2 = 0.032$, $P = 0.405$) or the air–water temperature difference ($r^2 = 0.037$, $P = 0.370$) of the Phillips and Irbe classes. These results suggest that discrepancies between MOST and calibrated α values may have been at least partially

caused by the classification scheme of Phillips and Irbe. Their classification scheme might have been improved using classes based on Ri_{b10}, and by using as the dependent variable temperature and dewpoint temperature modification relative to the initial air–water temperature or dewpoint temperature difference, as in Eq. 9. Still, the data of Phillips and Irbe represent an intensive field investigation of air temperature and humidity modification over the Great Lakes that is unique in its spatial and seasonal coverage, and it was possible to extract useful information on IBL development from it through application of the IBLTE model. If a similar, unbinned dataset should become available in the future, it may be possible to obtain a more accurate parametrization of α by applying the classification approach described here.

4 Conclusion

A Lagrangian internal boundary-layer model was developed and applied to measurements of air temperature and humidity modification over water to obtain estimates of the internal boundary-layer growth rate coefficient, α, in coastal offshore flow under stable, neutral, and unstable conditions. A parametrization for α was developed using MOST. The MOST parametrization of α explained 78 and 61% of the variation in α obtained from the model under stable and unstable conditions, respectively, which was in close agreement under neutral conditions. Values of α obtained from both the models and the MOST parametrization were consistent with the Mulhearn (1981) parametrization, which are valid only for stable conditions. The parametrization described here is valid over a wide range in stability.

The MOST parametrization of α provides a means of estimating h in applications in which the complexity of a high-resolution numerical turbulence model is not warranted, or when the spatial resolution of a numerical scheme is too coarse to resolve the fine spatial scale of IBL development. For example, when making flux measurements in the coastal zone, it is useful to estimate whether the measurement platform is at a significant fraction of the IBL height to ensure that the flux is representative of the surface flux (e.g., Fairall et al. 2006). In addition, the parametrization of α in a model such as the IBLTE model can be used for estimating near-surface modification of gas mixing ratio and temperature, as well as the variation of surface fluxes and vertical gradients in the gas mixing ratio and temperature in coastal offshore flow.

Acknowledgements Funding was provided by the Great Lakes Commission and the NOAA's Health of the Atmosphere program. Reginald Hill of NOAA/ESRL provided the example for Matlab code for the analysis of the NEAQS data. Conversations with Richard E. Honrath contributed to the early development of the IBLTE model. David Phillips responded to inquiries regarding the availability of original data from the Phillips and Irbe (1978) article.

Appendix A: Mathematical Details of the IBLTE Model

The horizontal integral in Eq. 1 is evaluated numerically, applying the trapezoidal rule, at each fetch increment using the COARE algorithm to estimate the sensible and latent heat and the gas fluxes. The model is written here for a trace gas mixing ratio, but it is similarly applied to potential temperature and water vapour. It is necessary to model potential temperature to account for varying stability with fetch and also to calibrate the h parametrization using temperature and humidity modification data.

Wind speed determines the time required to travel a given fetch, and is therefore an important parameter in the integral depth scale. The 10-m wind speed overland is input into the model. Wind speed over water at 3-m height is determined using the empirical correlations for wind ratio of Phillips and Irbe (1978) as a function of fetch and initial air–water temperature difference. $\overline{U}$ is evaluated at each fetch increment by numerically integrating (five-point Gauss quadrature) the vertical profile of wind speed, $U(z)$ (roughness and stability dependent), given by the COARE algorithm:

$$\overline{U} = \frac{1}{h}\int_0^h U(z)\mathrm{d}z \tag{17}$$

A1. Initial Vertical Profiles Overland

The IBLTE model is intended to be implemented using surface-based measurements of overland temperature, humidity, and gas mixing ratio; therefore it is necessary to make assumptions regarding the initial vertical profiles of these variables overland. A lapse rate, γ, was added to allow for a non-adiabatic initial lapse rate for potential temperature or a linear gradient in mixing ratio across the mixed layer, as illustrated in Fig. 2:

$$\gamma = \gamma_\mathrm{e} - \gamma_\mathrm{d} \tag{18}$$

where γ_e is the environmental lapse rate and γ_d is the dry adiabatic lapse rate. For the general case in which soundings overland are not available, it is more reasonable to assume $\gamma_\mathrm{e} = -0.006\,\mathrm{K\,m^{-1}}$ for potential temperature and $\gamma = -0.001\,\mathrm{g\,kg^{-1}\,m^{-1}}$ for specific humidity, after the lowest two kilometres of the U.S. Standard Atmosphere, which is derived from many averaged soundings (reported in Seinfeld and Pandis 1998), than to assume the dry adiabatic lapse rate and a constant specific humidity with height. In application of the IBLTE model to other gases, a non-zero value of γ may be used, as for the example of water vapour, when the initial mixing ratio of the gas is height-dependent.

A2. Mathematical Approach to Profile Matching

The integral depth scale was divided into two parts, a lower and upper profile contribution (illustrated as the lower and upper shaded areas in Fig. 2).

$$H(x) = H(x)_\mathrm{l} + H(x)_\mathrm{u}. \tag{19}$$

The MOST profile contribution to the integral depth scale (lower shaded area in Fig. 2) is

$$H(x)_\mathrm{l} = \int_0^{z_\mathrm{m}} (r(z) - r_\mathrm{l})\,\mathrm{d}z + \frac{1}{2}\gamma z_\mathrm{m}^2 \tag{20}$$

in which the integral term was evaluated by numerical integration (Gauss quadrature) of the MOST profile. The term containing γ accounts for the contribution of the shaded area A at $z \le z_\mathrm{m}$ in Fig. 2.

The upper profile contribution is evaluated by re-arranging the z/h profile function and integrating after applying Eq. 3:

$$H(x)_u = h\,(r_\mathrm{s} - r_\mathrm{l})\int_{z_\mathrm{m}}^{h}\left[1 - \left(\frac{z}{h}\right)^n\right]\mathrm{d}\left(\frac{z}{h}\right), \tag{21}$$

which yields the following, after adding the lapse rate contribution (shaded area A in Fig. 2):

$$H(x)_u = h\,(r_s - r_l)\left[\frac{n - nf - f + f^{n+1}}{n+1}\right] + \frac{1}{2}\gamma\left(h^2 - z_m^2\right). \tag{22}$$

Equation 22 can be re-arranged to obtain r_s as a function of $H(x)_u$ and known variables.

In summary, the prediction of state variables (θ, water vapour, and gas mixing ratio) as a function of x and z involves an iterative determination of r_s to define the shape of the profile at $z_m < z < h$, subject to two constraints: (1) the profile modification integrated from $0 < z < h$, is equal to the surface flux integrated over the fetch, as in Eq. 1 and Fig. 2, and (2) a matching value of θ is given at z_m by the MOST flux-profile relations and Eq. 5. The approach is outlined below:

(1) Inputs: water surface temperature, overland values of state variables and U
   (a) Trace gas inputs: aqueous concentration, Henry's Law constant, molecular mass, molar volume;
   (b) Ancillary estimated inputs: downwelling longwave and shortwave irradiance, environmental lapse rate, Eq. 18, for state variables.

(2) Assign a value for α.

(3) Fetch loop
   (a) Update fetch, update h (Eq. 2), update U using empirical correlations (Phillips and Irbe 1978);
   (b) Call the COARE algorithm to determine the surface fluxes and turbulence scaling parameters, and determine $\overline{U}$ (Eq. 17);
   (c) Determine $H(x)$ for state variables by Eq. 1, right-hand side;
   (d) Profile matching loop (iterate until θ given by MOST flux-profile relations and Eq. 5 converge at z_m):
      (i) Evaluate $H(x)_l$, Eq. 20,
      (ii) Determine $H(x)_u$ by difference, Eq. 19,
      (iii) Determine r_s by Eq. 22, written for θ,
      (iv) Determine θ at z_m, Eq. 5,
      (v) Repeat steps i through iv for additional state variables,
      (vi) Call COARE using updated values of state variables at z_m,
      (vii) Test for convergence among MOST profile and Eq. 5 at z_m.
   (e) Update the state variables at z_m, repeat fetch loop.

References

Angevine W, Hare J, Fairall C, Wolfe D, Hill R, Brewer W, White A (2006a) Structure and formation of the highly stable marine boundary layer over the Gulf of Maine. J Geophys Res 111:D23S22. doi:10.1029/2006JD007465

Angevine WM, Tjernstrom M, Zagar M (2006b) Modeling of the coastal boundary layer and pollutant transport in New England. J Appl Meteorol 45:137–154

Blomquist BW, Fairall CW, Huebert BJ, Kieber DJ, Westby GR (2006) DMS sea–air transfer velocity: direct measurement by eddy covariance and parameterization based on the NOAA/COARE gas transfer model. Geophys Res Lett 33:1–4

Craig R (1946) Measurements of temperature and humidity in the lowest 1000 feet of the atmosphere over Massachusetts Bay. Pap Phys Oceanogr Meteorol 10:1–47

Croley TE II (1989) Verifiable evaporation modeling on the Laurentian Great Lakes. Water Resour Res 25(5):781–792

Croley TE, Hunter TS (1996) Great lakes monthly hydrologic data. Great Lakes Environmental Research Laboratory. http://ftp.glerl.noaa.gov/publications/tech_reports/glerl-083/UpdatedFiles/. Accessed 9 October 2009

Draxler R, Stunder B, Rolph G, Stein A, Taylor A (2009) HYSPLIT (Hybrid single-particle Lagrangian integrated trajectory) model, v. 4.9. National Oceanic and Atmospheric Administration Air Resources Laboratory. www.arl.noaa.gov/HYSPLIT.php. Accessed 9 October 2009

Environment Canada (2009) National climate data and information archive. http://climate.weatheroffice.ec.gc.ca/climateData/. Accessed 10 October 2009

Fairall CW, Hare JE, Edson JB, McGillis W (2000) Parameterization and micrometeorological measurement of air–sea gas transfer. Boundary-Layer Meteorol 96:63–105

Fairall CW, Bradley EF, Hare JE, Grachev AA, Edson JB (2003) Bulk parameterization of air–sea fluxes: updates and verification for the COARE algorithm. J Clim 16:571–591

Fairall CW, Bariteau L, Grachev AA, Hill RJ, Wolfe DE, Brewer WA, Tucker SC, Hare JE, Angevine WM (2006) Turbulent bulk transfer coefficients and ozone deposition velocity in the International Consortium for Atmospheric Research into Transport and Transformation. J Geophys Res 111:1–19

Garratt JR (1987) The stably stratified internal boundary layer for steady and diurnally varying offshore flow. Boundary-Layer Meteorol 38:369–394

Garratt JR (1990) The internal boundary layer—a review. Boundary-Layer Meteorol 50:171–203

Hsu SA (1989) A verification of an analytical formula for estimating the height of the stable internal boundary layer. Boundary-Layer Meteorol 48:197–201

Mahrt L (1999) Stratified atmospheric boundary layers. Boundary-Layer Meteorol 90:375–396

McGillis WR, Edson JB, Zappa CJ, Ware JD, McKenna SP, Terray EA, Hare JE, Fairall CW, Drennan W, Donelan M, DeGrandpre MD, Wanninkhof R, Feely RA (2004) Air–sea CO_2 exchange in the Equatorial Pacific. J Geophys Res 109:C08S02. doi:10.1029/2003JC002256

Melas D (1989) The temperature structure in a stably stratified internal boundary layer over a cold sea. Boundary-Layer Meteorol 48:361–375

Mulhearn P (1981) On the formation of a stably stratified internal boundary-layer by advection of warm air over a cooler sea. Boundary-Layer Meteorol 21:247–254

Perlinger JA, Tobias DE, Morrow PS, Doskey PV (2005) Evaluation of novel techniques for measurement of air–water exchange of persistent bioaccumulative toxicants in Lake Superior. Environ Sci Technol 39:8411–8419

Perlinger JA, Rowe MD, Tobias DE (2008) Atmospheric transport and air–water exchange of hexachlorobenzene in Lake Superior. Organohalogen Compd 70:598–601

Phillips DW, Irbe JG (1978) Land-to-lake comparison of wind, temperature, and humidity on Lake Ontario during the International Field Year for the Great Lakes (IFYGL). Atmospheric Environment Service, Environment Canada, Downsview, Ontario, 51 pp

Seinfeld JH, Pandis SN (1998) Atmospheric chemistry and physics. Wiley, New York, 1326 pp

Smedman A-S, Bergström H, Grisogono B (1997) Evolution of stable internal boundary layers over a cold sea. J Geophys Res 102(C1):1091–1099

Stull RB (1988) An introduction to boundary layer meteorology. Kluwer, Dordrecht, 670 pp

Taylor G (1915) Eddy motion in the atmosphere. Phil Trans Roy Soc London Ser A 215: 1–26. www.jstor.org/stable/91100